Correction of sun-sensor geometry effects from MODIS MCD43A1 product for tropical forest applications

Fabien Hubert Wagner[1,*]
Benjamin Brede [2]
Jan Verbesselt[2]
Luiz Eduardo Oliveira e Cruz de Aragão[1]

[1] Instituto Nacional de Pesquisas Espaciais – INPE
Caixa Postal 515 – 12245-970 – São José dos Campos - SP, Brasil
wagner.h.fabien@gmail.com, laragao@dsr.inpe.br

[2] Wageningen University of Environmental Sciences – Laboratory of Geo-information Science and Remote Sensing
6708PB – Wageningen – Netherlands
benjamin.brede@wur.nl, jan.verbesselt@wur.nl

* FAPESP, processo 13/14520-6

Abstract. Tropical forests have an important role in the terrestrial carbon (C) cycle. In the current context of atmospheric CO_2 increase, understanding how the forest react and feedback to this CO_2 increase is an urgent need. The production of leaves is an important part of the carbon cycle of tropical forest and is poorly known due to the difficulty of direct measurements. Vegetation indices from remote sensing represent an interesting tools to study this process. However, recent studies have highlight that the variations of EVI is largely due to sun-sensor geometry in tropical latitude. This article describes how to corrected reflectance for the sun-sensor geometry artefacts, a current prequisite to the computation of vegetation indices. We describe the step-by-step procedure to correct reflectances and to obtain corrected vegetation indices with the MODIS MCD43A1 and MCD43A2 product suite. Subsequently with give a pratical example of application in a tropical forest of French Guiana. Our results show that despite constant cloudy conditions, EVI corrected estimation is feasible considering a sufficient area of forest. Corrected EVI show a seasonal pattern unrelated with sun-sensor geometry. Based on field data of litterfall, we show that corrected EVI reflects the pattern of leaf production. Subsequently, we encourage to use EVI corrected for sun-sensor geometry to follow leaf phenology in tropical forests.

Keywords: tropical forest, phenology, remote sensing, EVI correction, reflectance correction, methodology

1. Introduction

Tropical forests have an important role in the terrestrial carbon (C) cycle. On one hand, 55% of the global forest C stock is stored in tropical areas (471±93 Pg C). On the other, carbon sequestration in tropical intact forests and in tropical regrowing forests account for more than 70% of the global gross forest sink, ≈4.0 PgC yr^{-1} (Pan et al., 2011; Baccini et al., 2012).

In plants, the balance of photosynthesis and respiration determines the storage rates of carbohydrates in woody tissues, which is the main component of carbon storage in the trees (Kozlowski, 1992). Tree growth occurs in two ways. Primary growth corresponds to the length extension of roots and shoots from the apical meristems, where the leaves grow. Secondary growth gathers all the biological mechanisms behind the stem growth in thickness (Kozlowski, 1992). These two production are seasonal, but today we need to understand (i) if this production are the result of a trade-off of carbon allocation in the plant as already observed in Bolivia

(Doughty et al., 2014); and (ii) what are the climate drivers of seasonal leaf and wood production to pave the way for more sophisticated seasonal carbon cycle models.

Whereas seasonal field measurements of wood production are feasible and now relatively known for tropical forests, seasonal field measurements of leaf production are difficult to made and there is a need for indirect measurement methods. Seasonality of leaf phenology was observed, mostly in the Amazon forest, from (i) field measurement of litterfall and leave production (Chave et al., 2010; Zalamea and Gonzalez, 2008; Bonal et al., 2008) and (ii) satellite measurements (Huete et al., 2006; Asner et al., 2004; Caldararu et al., 2012; Wagner et al., 2013). The latter studies observed leaf phenology through variations in vegetation index, i.e. Leaf Area Index (LAI), Normalized Difference Vegetation Index (NDVI) and Enhanced Vegetation Index (EVI) (Justice et al., 1998). From satellite measurements, productivity, reported in terms of increasing vegetation indices as a proxy for canopy photosynthetic capacity, is correlated with leaf production and peaked in dry season (Huete et al., 2006; Brando et al., 2010; Anderson, 2012; Wagner et al., 2013). These indices are computed with measurements of surface reflectance by sensors aboard satellites.

However, recent studies have highlight that the interpretation of vegetation index must be made carefully because reflectance used to compute vegetation indexes are sensitive to view-illumination effects due to the variation of the solar zenith angle and view angle of the measurement (Galvao et al., 2013; Morton et al., 2014). Some MODIS products with reflectance and vegetation indices corrected for solar angle and view angle already exists. The MODIS MCD43B1 product at spatial resolution of 1 km, is an example of these products and is expected to represent biological processes with higher fidelity and to resolve the problem of cloudy condition in the tropics. Nevertheless, for some applications, the computation of corrected reflectance at a spacial resolution of 500 m may be needed. MCD43A4 give reflectance for fixed view sensor angle, but sun angle is not fixed, and correspond to the angle at local solar noon. This reflectance corrections for sun and sensor view angle are today a prequisite to further analysis of vegetation index in the tropics. Studies working with corrected indices are very few (Brede et al., 2014; Morton et al., 2014) and the NASA documentations on this suject are sparse, dispersed and difficult, particularly for users who are not from the remote sensing fields.

The objective of this paper is to explain the basis of the correction of reflectance for the 7 bands (Table 1) of the the MCD43A1 product, and describe how users can make their own corrections, i.e. to model reflectance values from a fixed sensor and sun angle. Subsequently, we give a pratical example of corrected reflectances and vegetation index in a tropical forest site. The ultimate goal of this document is to provide a conceptual basis for every researcher who wish to understand how reflectance values and vegetation indices reflect biological functioning of the tropical forest.

Table 1: MODIS MCD43 bands, number and associated color names.

MODIS band wavelength (μm)	Modis band number	color
0.459 - 0.479	3	blue
0.545 - 0.565	4	green
0.620 - 0.670	1	red
0.841 - 0.876	2	NIR
1230 - 1250	5	–
1.628 - 1.654	6	–
2.105 - 2.155	7	–

2. Methods

This section compiled informations from recently published work (Brede et al., 2014) and from theorical articles for the correction of reflectance values (Schaaf et al., 2002, 2011; Lucht et al., 2000; Strahler and Muller, 1999; Roujean et al., 1992).

2.1. MCD43A1 BRDF model

The reflectance of surfaces is dependent on the observer direction relative to the position of the light source. The Bidirectional Reflectance Distribution Function (BRDF) expresses this dependency and can have complex forms. Scattering models take this into account and allow the modelling of Bidirectional Reflectance Factors (BRFs) at arbitrary view and sun zenith angles. In this sense, they allow to control for Sun-Sensor Geometry Effects (SSGEs). The two MODIS sensors aboard the Aqua and Terra satellites provide unique opportunities to calibrate the BRDF. Each one has a wide viewing angle, allowing a wide range of viewing geometries for each pixel, and produces images under a different sun zenith angle than the other one due to the morning (Terra) and afternoon (Aqua) local overpass time. These facts permit a wide spread angular sampling, i.e sample of pixel reflectance values for different sun and sensor view angles, which is necessary to statistically fit the land surface BRDF.

The MCD43A1 product suite contains results of fitting pixel-wise reflectance observations of 16 days to a semi-empirical, linear BRDF model, the RossThick-LiSparse-Reciprocal (RTLSR) model (Schaaf et al., 2002, 2011). This kernel based model consists of three terms, which each characterise different surface scattering processes (Lucht et al., 2000). The first parameters, the isotropic parameter f_{iso}, describes Lambertian reflectance. This model assumes a constant diffuse reflection which is an intrinsic property of the surface independant of sun and observation geometry. The second parameter, the volumetric parameter f_{vol}, describes intra-crown volume scattering by leaves in the canopy and is sensitive to leaf optical properties and their spatial density. The third parameter, the geometric parameter f_{geo}, describes shadowing effects of canopy gaps or protrusions. While the isotropic term is not dependent on sun and observation geometry, the volumetric and geometric terms are functions of sun and viewing geometry.

The model is calibrated for each band λ separately and parameters f_{iso}, f_{vol} and f_{geo} are returned for each of the 7 bands of Modis (Table 1). In the MCD43A1, for the 1 and for a given pixel, the product give f_{iso}, f_{vol} f_{geo}, in this order (`https://lpdaac.usgs.gov/products/modis_products_table/mcd43b1`). For a given band, with these three parameters (f_{iso}, f_{vol}, f_{geo}), and θ_s the solar zenith angle, θ_v the view zenith angle, and relative azimuth angle ϕ, the corrected reflectances can be computed. θ_s, θ_v and ϕ have to be chosen by the user. A common setting is to model the sensor position at nadir (θ_v=0), so that ϕ=0.

The corrected reflectance, i.e. the Bidirectional Reflectance Factor (BRF), is modelled as a linear combination of the kernel terms:

$$BRF(\theta_s, \theta_v, \phi, \lambda) = f_{iso}(\lambda) + f_{vol}(\lambda)K_{vol}(\theta_s, \theta_v, \phi, \lambda) + f_{geo}K_{geo}(\theta_s, \theta_v, \phi, \lambda) \quad (1)$$

where BRF is the Bidirectional Reflectance Factor (i.e. the value of corrected reflectance) at view zenith angle θ_v, solar zenith angle θ_s and relative azimuth angle ϕ. The parameters f_{iso}, f_{vol} and f_{geo}, given in MCD43A1 product, represent reflectances (Roujean et al., 1992) and are scaled according to the kernel values K_{vol} and K_{geo}. These kernel values have to be computed by the user, the details are given in the following sections.

2.1.1. Computation of the volumetric RossThick kernel, K_{vol}

The volumetric RossThick kernel K_{vol} assumes a dense leaf canopy (Roujean et al., 1992). It models the canopy as a homogenous medium with randomly oriented facets. The kernel is computed as following (Strahler and Muller, 1999).

With ξ the angle between sun and sensor defined as :

$$\cos \xi = \cos \theta_s \cos \theta_v + \sin \theta_s \sin \theta_v \cos \phi \tag{2}$$

where θ_s the solar zenith angle, θ_v the view zenith angle, and relative azimuth angle ϕ, K_{vol} is computed as :

$$K_{vol}(\theta_s, \theta_v, \phi) = \frac{(\frac{\pi}{2} - \xi) \cos \xi + \sin \xi}{\cos \theta_s + \cos \theta_v} - \frac{\pi}{4} \tag{3}$$

Generally the user's want to have at nadir view, i.e. ϕ=0, relative azimuth angle ϕ in this case have no effect ($\cos(\phi) = 1$, equation 2).

2.1.2. Computation of the geometric, reciprocal LiSparse kernel K_{geo}

The geometric, reciprocal LiSparse kernel K_{geo} assumes a sparse leaf canopy, i.e. non-overlapping shadows cast by randomly distributed objects. For MODIS processing the dimensionless crown relative height and shape parameter are defined as $\frac{h}{b} = 2$ and $\frac{b}{r} = 1$, respectively. This means that the tree crowns are modelled as spheres that are separated from the ground by half their diameter (Lucht et al., 2000). Here we detailed the different equations needed to compute K_{geo} and its formula (Lucht et al., 2000; Strahler and Muller, 1999):

$$\theta'_s = tan^{-1}(\frac{b}{r} \tan \theta_s), \quad \theta'_v = tan^{-1}(\frac{b}{r} \tan \theta_v) \tag{4}$$

$$\cos \xi' = \cos \theta'_s \cos \theta'_v + \sin \theta'_s \sin \theta'_v \cos \phi \tag{5}$$

$$D = \sqrt{\tan^2 \theta'_s + \tan^2 \theta'_v - 2 \tan \theta'_s \tan \theta'_v \cos \phi} \tag{6}$$

$$\cos t = \frac{h}{b} \frac{\sqrt{D^2 + (\tan \theta'_s \tan \theta'_v \sin \phi)^2}}{\sec \theta'_s \sec \theta'_v}, \quad t = \sec(\min(\max(\cos t, -1), 1)) \tag{7}$$

$$O(\theta_s, \theta_v, \phi) = \frac{1}{\pi}(t - \sin t \cos t)(\sec \theta'_s + \sec \theta'_v) \tag{8}$$

With the equations 4, 5, 6, 7 and 8, K_{geo} can be compute as :

$$K_{geo}(\theta_s, \theta_v, \phi) = O(\theta_s, \theta_v, \phi) - \sec \theta'_s - \sec \theta'_v + \frac{1}{2}(1 + \cos \xi') \sec \theta'_v \sec \theta'_s \tag{9}$$

2.1.3. Quality of the BRDF parametrisation

Quality indices for MCD43A1 data are available in the MCD43A2 product suite. This dataset contains quality indices of the fit of BRDF for pixels and each reflectance bands named BRDF_Albedo_Band_Quality, Table 2 (Lpdaac-NASA, 2013). Full inversions indicates that there was a sufficient number of high-quality directional observations for the statistical fitting of the BRDF model. When only few observations are available, a back-up algorithm offers model inversions, termed magnitude inversion. This algorithm makes use of the BRDF properties of previous full inversions and scales these shapes to new measurements.

Table 2: MODIS MCD43A2 quality index value and associated description.

Quality Index	Interpretation
0	Best quality, 75% or more with best full inversions
1	Good quality, 75% or more with full inversions
2	Mixed,75% or less full inversions and 25% or less fill-values
3	All magnitude inversions or 50% or less fill-values
4	50% or more fill-values
255	Fill-values

2.2. Application for a tropical forest

In this article, we give an example for a subset of the tile h12v08 from MCD43A1 product on the period 2007-2010. The subset is a square of 40 km side, centered on the Paracou forest site, 5°16'28"N, 52°55'25"W. The selection of forested pixels was made with freely available tree cover data and tree cover change 2000 and 2012 at 30 m spatial resolution based on Landsat images (Hansen et al., 2013). Forest type was assumed to be the same in all forested pixels. The view angle θ_v was fixed at 0° and sun zenith angle θ_s at 30° and relative azimuth angle ϕ at 0. Only pixels with quality from 0 to 3 were retained in the analysis (quality index was extracted from MCD43A2 product, Table 2). BRDF-corrected EVI was then computed with corrected reflectance, equation 10. Uncorrected EVI and litterfall were estimated in a companion study (Wagner et al., 2013). BRDF-corrected EVI and NBAR EVI are given as averages of the selected pixels by quality index amongst the 3122 forested pixels of the sample area. Solar zenith angles at local noon were extracted from the band BRDF_Albedo_Ancillary of the MCD43A2 product. All analysis were performed in R (Team, 2014).

$$EVI = 2.5 \times \frac{\rho_{NIR} - \rho_{red}}{\rho_{NIR} + 6\rho_{red} - 7.5\rho_{blue} + 1} \tag{10}$$

3. Results and discussion - Example of BRDF-corrected EVI time serie

3.1. Quality of BRDF

Mean of valid MCD43 observations of BRDF-corrected EVI is of 20.3%(annual) and range from 0 to 60.25% (Fig. 1f). Due to the seasonality of the site, high quantity of valid observations are mostly encoutered during the dry season (July to November) when cloud cover is low. However, due to our spatial sample (3122 forested pixels), 1% of valid observations represents $\approx$ 31 pixels, which is reasonable for the estimation EVI in this homogenous forest, classified as a high forest with regular canopy (Gond et al., 2011).

3.2. Temporal pattern of EVI

Temporal variation of BRDF-corrected, NBAR and uncorreted EVI are presented in the Fig. 1a, 1b and 1c. The BRDF-corrected and NBAR EVI are highly correlated (pearson ρ=0.96, p<0.001) and show only minor differences. The peak of BRDF-corrected EVI is smoother and do not reach the maximal values of NBAR EVI peaks. BRDF-corrected EVI and NBAR EVI have a seasonal pattern with an increase in the dry season (July to November), (Fig. 1) with a maximum reached before the onset of the wet season (December to January), followed by a decrease during the wet season. Uncorrected EVI, (Fig. 1c), is correlad with both BRDF-corrected EVI and NBAR EVI (respectively, pearson ρ=0.30, p=0.0163; ρ=0.26, p=0.038). A statistically significant seasonality exists in EVI irrespective of the processing type (cosinor test: BRDF-corrected EVI, p<0.05; NBAR EVI, p<0.05; uncorrected EVI, p<0.05). Only
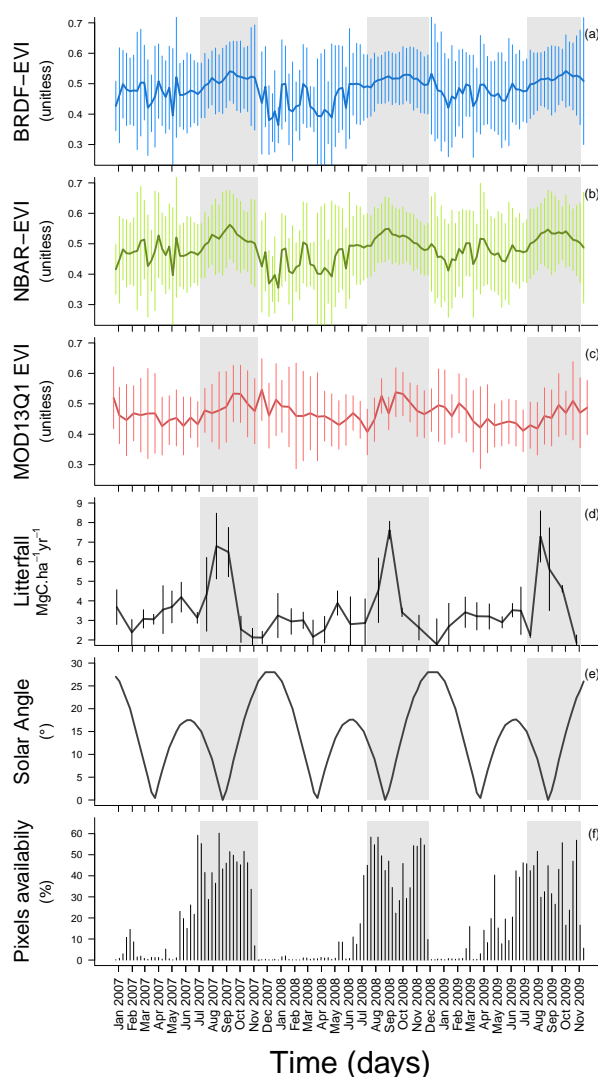
Figure 1: Temporal variations of spatially averaged BRDF-corrected EVI (a), NBAR EVI (b); uncorrected EVI (c); litterfall production at the Paracou site(d); solar zenith angle (d) and pourcentage of valid MCD43A1 observations for the estimations of averaged BRDF-corrected EVI and NBAR EVI. Grey bands indicate dry seasons (typically July to November). The x-axis tick-marks indicate the middle of the month.

NBAR EVI have a significant correlation with solar zenith angle, (Fig. 1e) (pearson ρ=-0.36, p<0.001; BRDF-corrected EVI, pearson ρ=-0.10, p=0.24; uncorrected EVI, pearson ρ=0.14, p=0.26). When corrected only for view sensor angle (EVI NBAR), the correlation with solar angle appeared. It seems that the BRDF correction succeed to suppress the effect of solar angle variations on reflectance values. Our results are not in accordance with the results of Morton et al. (2014) and indicate a greening for this forest in the dry season even after correction of sun-sensor geometry effects.

3.3. Ecological significance of EVI increase

At the onset of the dry season, BRDF-corrected EVI increased when the peak of litterfall was observed (Fig. 1d). At Paracou, as expected for an evergreen tropical forest, leaf litter is produced throughout the year, indicating that the trees have sufficient carbon supply and adequate climate to produce new leaves even at the beginning of the dry season when litterfall

peaks, 1d. Peaks of BRDF-corrected EVI occurred 1 to 2 months after litterfall peak. Data on leaf maturation in tropical forest are very sparse, but some study have showed that leaf maturation for tropical trees (leaf expansion and photosynthetic development) can occurs in 15-40 days (Cai et al., 2005; Kursar and Coley, 1991). This process could explained the lag between litterfall peak and EVI peak. The ecological significance of a so-called "forest-greening" (Huete et al., 2006) in French Guiana is leaf production, which mainly occurs in the dry season when old leaves are replaced, i.e. when litterfall peaks, (Fig.1d). The plants are ready with fully-developed foliage to take advantage of favourable wet conditions for wood production, by the onset of the wet season (Wagner et al., 2014).

4. Conclusions

Our result confirm the link between intra-annual variations of EVI and field observations of leaf phenology and suggest that most leaves are shed when new ones appear. Therefore, in tropical forests, we suggest that BRDF-corrected EVI could be use to follow-up the phenology and to help understanding the drivers controling this important process of the carbon cycle.

Acknowledgements

References

Anderson, L. O. Biome-Scale Forest Properties in Amazonia Based on Field and Satellite Observations. *Remote Sensing*, 4, p. 1245–1271, 2012.

Asner, G. et al. Drought stress and carbon uptake in an Amazon forest measured with spaceborne imaging spectroscopy. *Proceedings of the National Academy of Sciences of the United States of America*, 101, p. 6039–6044, 2004.

Baccini, A. et al. Estimated carbon dioxide emissions from tropical deforestation improved by carbon-density maps. *Nature Climate Change*, 2, p. 182–185, 2012.

Bonal, D. et al. Impact of severe dry season on net ecosystem exchange in the Neotropical rainforest of French Guiana. *Global Change Biology*, v. 14, p. 1917–1933, 2008.

Brando, P. M. et al. Seasonal and interannual variability of climate and vegetation indices across the Amazon. *Proceedings of the National Academy of Sciences of the United States of America*, 107, p. 14685–14690, 2010.

Brede, B. et al. *Performance of the Enhanced Vegetation Index to Detect Inner-annual Dry Season and Drought Impacts on Amazon Forest Canopies*. Thesis (Master) — Wageningen University and Research Centre, 2014.

Cai, Z.-Q. et al. Leaf development and photosynthetic properties of three tropical tree species with delayed greening. *Photosynthetica*, v. 43, p. 91–98, 2005.

Caldararu, S. et al. Inferring Amazon leaf demography from satellite observations of leaf area index. *Biogeosciences*, 9, p. 1389–1404, 2012.

Chave, J. et al. Regional and seasonal patterns of litterfall in tropical South America. *Biogeosciences*, 7, p. 43–55, 2010.

Doughty, C. E. et al. Allocation trade-offs dominate the response of tropical forest growth to seasonal and interannual drought. *ECOLOGY*, 95, p. 2192–2201, 2014.

Galvao, L. S. et al. View-illumination effects on hyperspectral vegetation indices in the Amazonian tropical forest. *International Journal of Applied Earth Observation and Geoinformation*, 21, p. 291–300, 2013.

Gond, V. et al. Broad-scale spatial pattern of forest landscape types in the Guiana Shield. *International Journal of Applied Earth Observation and Geoinformation*, 13, p. 357–367, 2011.

Hansen, M. C. et al. High-resolution global maps of 21st-century forest cover change. *Science*, v. 342 (6160), p. 850–853, 2013.

Huete, A. R. et al. Amazon rainforests green-up with sunlight in dry season. *Geophysical Research Letters*, v. 33, 2006.

Justice, C. et al. The Moderate Resolution Imaging Spectroradiometer (MODIS): Land remote sensing for global change research. *IEEE Transactions on Geoscience and Remote Sensing*, 36, p. 1228–1249, 1998.

Kozlowski, T. Carbohydrate sources and sinks in woody-plants. *Botanical Review*, 58, p. 107–222, 1992.

Kursar, T.; Coley, P D. Nitrogen content and expansion rates of young leaves of rain forest species: implications for herbivory. *Biotropica*, v. 23, p. 141–150, 1991.

Lpdaac NASA. *MODIS Land Products Quality Assurance Tutorial: Part-4 . How to interpret and use MODIS QA information in the BRDF and Albedo product suite*. [S.l.], 2013.

Lucht et al., A. An algorithm for the retrieval of albedo from space using semiempirical brdf models. *IEEE Transactions on Geoscience and Remote Sensing*, v. 38 (2), p. 977–998, 2000.

Morton, D. C. et al. Amazon forests maintain consistent canopy structure and greenness during the dry season. *NATURE*, 506, p. 221+, 2014.

Pan, Y. et al. A Large and Persistent Carbon Sink in the World's Forests. *Science*, 333, p. 988–993, 2011. ISSN 0036-8075.

Roujean, J.-L. et al. A bidirectional reflectanceectance model of the earth's surface for the correction of remote sensing data. *Journal of Geophysical Research*, v. 97(D18), p. 20455, 1992.

Schaaf, C. B. et al. First operational brdf, albedo nadir reflectance products from modis. *Remote Sensing of Environment*, v. 83 (1-2), p. 135–148., 2002.

Schaaf, C. B. et al. Aqua and terra modis albedo and reflectance anisotropy products. In: Ramachandran, B.; Justice, C. O.; Abrams, M. J. (Ed.). *Land Remote Sensing and Global Environmental Change - NASA's Earth Observing System and the Science of ASTER and MODIS*. [S.l.]: New York, Dordrecht, Heidelberg, London: Springer, 2011. cap. 23, p. 579–602.

Strahler, A. H.; Muller, J.-P. *MODIS BRDF/Albedo Product: Algorithm theoretical basis document version 5.0*. [S.l.], 1999.

Team, R. C. *R: A Language and Environment for Statistical Computing*. Vienna, Austria, 2014.

Wagner, F. et al. Pan-tropical analysis of climate effects on seasonal tree growth. *PLoS ONE*, v. 9, 2014.

Wagner, F. et al. Asynchronism in leaf and wood production in tropical forests: a study combining satellite and ground-based measurements. *Biogeosciences*, v. 10, p. 7307–7321, 2013.

Zalamea, M.; Gonzalez, G. Leaffall phenology in a subtropical wet forest in Puerto Rico: From species to community patterns. *Biotropica*, 40, p. 295–304, 2008.